Aalborg Universitet

Stark effect in spherical quantum dots

Pedersen, Thomas Garm

Stark effect in spherical quantum dots

Thomas Garm Pedersen[*]

Department of Materials and Production, Aalborg University, DK-9220 Aalborg Øst, Denmark

The Stark problem in quantum-confined geometries is challenging in high fields. In particular, the localization of electrons near sample boundaries is hard to accurately capture in perturbation methods. We analyze the problem for spherical quantum dots using a combination of numerical diagonalization and analytical perturbation approaches. Closed-form expressions for polarizabilities and hyperpolarizabilities of arbitrary states are obtained. In addition, a hypergeometric resummation ansatz replicating the correct high-field behavior is constructed. We find that a simple resummation approach is superior to even 14th-order perturbation series.

I. INTRODUCTION

The Stark effect is a powerful tool for characterization and manipulation of electronic systems. Similarly, it is a theoretical challenge requiring accurate perturbation theories. A wide range of quantum structures have been analyzed, including hydrogen atoms in three and other dimensions [1–5], quantum wells and wires [6–8], and quantum dots [9–17]. The last group encompasses various quantum structures with three-dimensional confinement. Prominent examples count spherical or hemispherical nanoparticles [9–15] and planar graphene dots [16,17]. In photo-excited nanostructures, excitons play a crucial role, and their Stark shifts have been studied in detail [13–15,18–20].

Theoretical studies of Stark shifts are typically based on elaborate numerical perturbation techniques or, occasionally, variational approaches. However, in sufficiently simple geometries, analytical studies are feasible, especially if only low-order corrections are sought. In symmetric structures placed in a field F, the Stark shift of nondegenerate states is approximately given by $E(F) - E(0) \approx -\frac{1}{2}\alpha F^2$, where $E(F)$ is the field-dependent energy and α is the polarizability. The Dalgarno-Lewis technique [21] is ideally suited for analytical calculations of α, as documented in several cases [8,17,22–25]. In principle, higher order corrections can be computed by repeated application of this technique. Such high-order computations, however, have rarely been attempted, and, for hydrogen atoms, alternative methods have been applied [2–5]. Obviously, higher order corrections are required in strong field cases. In particular, in quantum-confined geometries, strong fields tend to localize electrons near the sample boundary. This phenomenon is particularly difficult to capture in perturbation expansions. Recently, however, "resummation" methods have been developed to extend the validity of (divergent) perturbation series to arbitrary field strengths [26,27]. Parametrization of such resummation methods typically requires access to several low-order terms. In the case of metastable states, an important feature of the resummed

series using branch-cut selected functions is that the ionization rate emerges automatically as the imaginary part of the energy [26,27]. This highly nonperturbative phenomenon cannot be captured by any finite perturbation series [28].

In the present work, we revisit the Stark problem in spherical quantum dots. We will demonstrate that the Dalgarno-Lewis technique is readily applied to obtain a high-order perturbation series in the applied field for, in fact, any state. In particular, simple analytical expressions for the polarizability and lowest hyperpolarizability are found for all states. Moreover, for the ground state we find corrections up to 14th power in the field. We then turn to hypergeometric resummation [27] to extend the perturbation series to high-field scenarios. By incorporating the exact infinite-field limit, we provide an extremely accurate resummed series. All analytical results are verified by comparison with numerical eigenvalues based on diagonalization in a large, finite basis.

II. STARK EFFECT

To achieve the above-mentioned goals, we clearly need to limit the analysis to a sufficiently simple model. Hence, we consider a single electron in a spherical quantum well with infinite barriers, as illustrated in Fig. 1. We, thus, ignore many-body effects as well as spill-out into the surrounding material. The single-particle approximation is accurate in the case of small, strongly confining nanoparticles, for which Coulomb effects are a minor correction. Similarly, the infinite barrier is appropriate for nanoparticles suspended in liquids or air, but not necessarily for quantum dots embedded in a semiconducting host. Also, the model is not applicable to metallic nanoparticles, in which screening via redistribution of electrons in the field is essential. It is convenient to use units, in which $e = \hbar = m_e = a = 1$ with m_e the effective electron mass and a the nanoparticle radius. These then differ from atomic units by choosing (1) effective rather than free-electron mass and (2) nanoparticle rather than Bohr radius as mass and distance units, respectively. Hence, the full eigenvalue problem is simply

$$\left\{-\tfrac{1}{2}\nabla^2 + Fr\cos\theta\right\}\varphi(\vec{r}) = E\varphi(\vec{r}), \tag{1}$$

————————
[*]tgp@mp.aau.dk
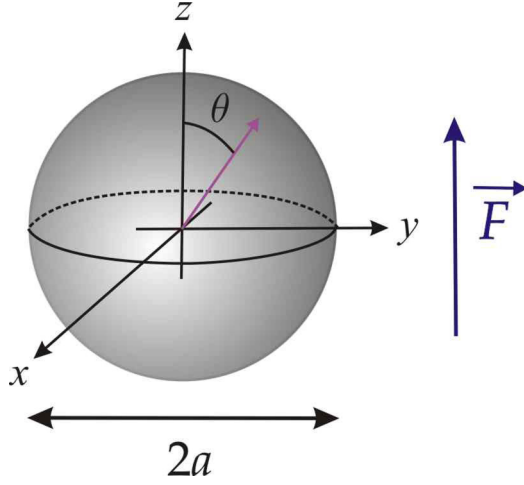
FIG. 1. Nanosphere of radius a perturbed by a vertical field $\vec{F}$.

supplemented by the Dirichlet boundary condition requiring a vanishing wave function at $r = 1$. The electric field is now in units of $F_0 = \hbar^2/(em_e a^3)$ and polarizabilities α and first hyperpolarizabilities β are in units of $\alpha_0 = e^2 m_e a^4/\hbar^2$ and $\beta_0 = e^4 m_e^3 a^{10}/\hbar^6$, respectively. The unperturbed eigenstates and associated energies are then

$$\varphi_{nlm}^{(0)}(\vec{r}) = Y_l^{(m)}(\theta, \phi) N_{nl} j_l(\lambda_{ln} r),$$

$$N_{nl} = \frac{\sqrt{2}}{j_{l+1}(\lambda_{ln})}, \quad E_{nl}^{(0)} = \frac{\lambda_{ln}^2}{2}. \tag{2}$$

Here $Y_l^{(m)}$ is a spherical harmonic and j_l the lth spherical Bessel function, for which λ_{ln} is the nth zero, i.e., $j_l(\lambda_{ln}) = 0$ with eigenstate index $n = 1, 2, 3, \ldots$. A simple but excellent approximation for the zeros is given by McMahon's formula [29] $\lambda_{ln} \approx \frac{\pi}{2}(l + 2n) - \frac{1}{\pi} l(l + 1)/(l + 2n)$, but throughout we use the numerically determined roots.

The field dependence of the eigenvalues in Eq. (1) can be found either by numerical diagonalization of an expansion in an appropriate basis or by perturbative means. In the present work, both approaches are applied and compared. Moreover,

below we use hypergeometric resummation to convert the finite perturbation series of the ground state to a more generally applicable result. By choosing the field direction as the polar axis, the perturbation does not couple different m values, which remain good quantum numbers. In contrast, the field couples angular momenta l according to

$$\cos\theta Y_l^{(m)}(\theta, \phi) = \beta_l Y_{l-1}^{(m)}(\theta, \phi) + \beta_{l+1} Y_{l+1}^{(m)}(\theta, \phi),$$

$$\beta_l = \sqrt{\frac{l^2 - m^2}{4l^2 - 1}}. \tag{3}$$

In our numerical diagonalization approach, we use the unperturbed eigenstates as basis functions. Hence, it follows from Eqs. (2) and (3) that the matrix elements of the coupling are

$$\langle \varphi_{nlm}^{(0)}(\vec{r}) | Fr\cos\theta | \varphi_{n'l'm}^{(0)}(\vec{r}) \rangle$$

$$= 4F(\delta_{l',l-1}\beta_l + \delta_{l',l+1}\beta_{l+1}) \frac{\lambda_{ln}\lambda_{l'n'}}{\left(\lambda_{ln}^2 - \lambda_{l'n'}^2\right)^2}. \tag{4}$$

In practice, a basis restricted to $|m| \leqslant l \leqslant 30 + |m|$ and $1 \leqslant n \leqslant 30$ is applied for each m value. The resulting 930 dimensional matrix can, thus, be constructed analytically but must be diagonalized numerically.

Alternatively, the field dependence of the eigenvalues can be computed using perturbation theory. Traditionally, this involves complicated sum-over-states expressions. Whenever analytical corrections are sought, however, the Dalgarno-Lewis technique [21] is usually preferable. This approach relies on expanding wave functions and energies in Eq. (1) according to $\varphi = \varphi^{(0)} + \varphi^{(1)} + \cdots$ and $E = E^{(0)} + E^{(2)} + \cdots$, where the superscript indicates the order, i.e., power, of the perturbation. Note that only even orders appear in the energy due to the symmetry of the unperturbed problem. By collecting terms of identical order, the perturbed wave function is obtained order by order. In turn, corrections to the energy follow from the wave function. The technique is readily illustrated for the first-order correction to the wave function. We write $\varphi_{nlm}^{(1)}(\vec{r}) = F N_{nl}[\beta_l Y_{l-1}^{(m)}(\theta, \phi) R_{l-1}(r) + \beta_{l+1} Y_{l+1}^{(m)}(\theta, \phi) R_{l+1}(r)]$. Collecting first-order terms for each spherical harmonic, this leads to the inhomogeneous first-order equations

$$\left\{ -\frac{1}{2}\left(\frac{1}{r}\frac{\partial^2}{\partial r^2}r - \frac{l(l-1)}{r^2} \right) - E_{nl}^{(0)} \right\} R_{l-1} + r j_l(\lambda_{ln} r) = 0,$$

$$\left\{ -\frac{1}{2}\left(\frac{1}{r}\frac{\partial^2}{\partial r^2}r - \frac{(l+1)(l+2)}{r^2} \right) - E_{nl}^{(0)} \right\} R_{l+1} + r j_l(\lambda_{ln} r) = 0. \tag{5}$$

Once these are solved, the second-order correction to the energy is obtained from

$$E_{nlm}^{(2)} = \langle \varphi_{nlm}^{(0)}(\vec{r}) | Fr\cos\theta | \varphi_{nlm}^{(1)}(\vec{r}) \rangle = F^2 N_{nl}^2 \int_0^\infty j_l(\lambda_{ln} r)\left\{ \beta_l^2 R_{l-1}(r) + \beta_{l+1}^2 R_{l+1}(r) \right\} r^3 dr. \tag{6}$$

The solutions to Eq. (5) correctly satisfying the boundary condition are readily shown to be

$$R_{l-1}(r) = \frac{1}{2\lambda_{ln}}\{(2l+1)r^{-1} j_l(\lambda_{ln} r) - (1 - r^2) j_{l+1}(\lambda_{ln} r)\},$$

$$R_{l+1}(r) = -\frac{1}{2\lambda_{ln}}\{(2l+1)r j_l(\lambda_{ln} r) + (1 - r^2) j_{l+1}(\lambda_{ln} r)\}. \tag{7}$$

In turn, the energy correction in terms of $L^2 = l(l+1)$ becomes

$$E_{nlm}^{(2)} = \frac{F^2}{24\lambda_{ln}^4}\left\{8L^2 - 3 - 12m^2 - 4\lambda_{ln}^2\frac{2L^2 - 3 + 6m^2}{4L^2 - 3}\right\}. \tag{8}$$

Incidentally, this result can be shown to agree with the standard sum-over-states perturbation approach using sum rules for Bessel zeros [30]:

$$E_{nlm}^{(2)} = 32F^2\sum_{n'=1}^{\infty}\left\{\beta_l^2\frac{\lambda_{ln}^2\lambda_{l-1,n'}^2}{\left(\lambda_{ln}^2 - \lambda_{l-1,n'}^2\right)^5} + \beta_{l+1}^2\frac{\lambda_{ln}^2\lambda_{l+1,n'}^2}{\left(\lambda_{ln}^2 - \lambda_{l+1,n'}^2\right)^5}\right\}$$

$$= 32F^2\left\{\beta_l^2\frac{(l-\frac{1}{2})(l+\frac{3}{2})(l+\frac{5}{2}) + \frac{1}{2}\lambda_{ln}^2(4l+1)}{96\lambda_{ln}^4} - \beta_{l+1}^2\frac{(l-\frac{3}{2})(l-\frac{1}{2})(l+\frac{3}{2}) + \frac{1}{2}\lambda_{ln}^2(4l+3)}{96\lambda_{ln}^4}\right\}. \tag{9}$$

Inserting the expression for β_l, the agreement with Eq. (8) is readily established. The Dalgarno-Lewis approach can now be extended to higher orders. We use the notation φ_{nlm} to denote the field-dependent wave function that evolves from $\varphi_{nlm}^{(0)}$ as the field is increased. Hence, $\lim_{F\to 0}\varphi_{nlm} = \varphi_{nlm}^{(0)}$. Note, however, that the angular momentum l is not a good quantum number in the presence of the field. We write

$$\varphi_{nlm}(\vec{r}) = \sum_{q=0}^{\infty}F^q\sum_{l'=l-q}^{l+q}Y_{l'}^{(m)}(\theta,\phi)\{f_{l'}^{(q)}(r)j_l(\lambda_{ln}r) + (1-r^2)g_{l'}^{(q)}(r)j_{l+1}(\lambda_{ln}r)\}. \tag{10}$$

Here l' increases in steps of two in the summation. Note that the orders l and $l+1$ of the spherical Bessel functions as well as the roots λ_{ln} pertain to the angular momentum of the unperturbed wave function, i.e., l rather than l'. The unknown radial functions turn out to be simple finite sums of powers:

$$f_{l'}^{(q)}(r) = \sum_{p=1-|l-l'+1|}^{q+2\lfloor q/2\rfloor}a_p^{(q)}r^p, \quad g_{l'}^{(q)}(r) = \sum_{p=1-|l-l'|}^{q-1+2\lfloor(q-1)/2\rfloor}b_p^{(q)}r^p. \tag{11}$$

Here, again, it is understood that p increases in steps of two; i.e., the powers r^p are either all even or all odd. Generally, the sums include both positive and negative powers. In addition, $\lfloor\cdots\rfloor$ is the floor function such that $\lfloor a/b\rfloor$ denotes the integer division ("div") operation. In this manner, the fourth-order energy correction becomes

$$E_{nlm}^{(4)} = \frac{F^4}{72\lambda_{ln}^{10}}\left\{32L^4 - 3L^2(61 + 44m^2) + 9(6 + 37m^2 + 12m^4) + 6\lambda_{ln}^2\frac{12 - 35L^2 - 16L^4 + 3(27 + 4L^2)m^2 + 12m^4}{4L^2 - 3}\right.$$

$$+ 4\lambda_{ln}^4\frac{54 - 20L^6 - 189m^4 + L^4(243 - 552m^2) - 9L^2(23 - 14m^2 - 92m^4)}{(4L^2 - 3)^2(4L^2 - 15)}$$

$$\left.+ 72\lambda_{ln}^6\frac{3 - 4L^6 + 30m^2 - 33m^4 + 3L^4(5 + 8m^2) - L^2(17 + 26m^2 + 20m^4)}{(4L^2 - 3)^3(4L^2 - 15)}\right\}. \tag{12}$$

The second- and fourth-order corrections provide, respectively, the polarizability $\alpha_{nlm} = -2E_{nlm}^{(2)}/F^2$ and hyperpolarizability $\beta_{nlm} = -4E_{nlm}^{(4)}/F^4$. Beyond fourth order, the higher orders quickly lead to exceedingly complicated expressions. For s-states with $l = m = 0$ including the ground state, however, reasonably compact results are found. Hence, in the Appendix, we provide expressions for the general s-state energy correction including terms up to 8th order and up to 14th order for the ground state.

III. NUMERICAL AND ANALYTICAL RESULTS

To validate our analytical expressions, we compare with numerical diagonalization results. As the m quantum numbers do not couple, we can obtain results for each value separately. In Fig. 2 we have collected numerical diagonalization results for $|m| = 0$, 1, and 2. The unperturbed ground-state energy is

$E_{100}^{(0)} = \pi^2/2 \approx 4.935$, and the second lowest state is $E_{11m}^{(0)} \approx 10.095$ found for $m = 0, \pm 1$. The pattern of degeneracies is clearly illustrated by the zero-field values in Fig. 2. Once a nonvanishing field is considered, however, these degeneracies are lifted (a degeneracy between $m = \pm|m|$ remains, of course). Given the characteristic energy scale of the unperturbed levels, we expect low-order perturbation theory to break down around field strengths of the order $F \sim 10$. As will be demonstrated below, this is indeed the case.

Next, we turn to the perturbative results. The second- and fourth-order corrections in Eqs. (8) and (12), respectively, provide results valid for arbitrary $\{nlm\}$. As above, though, we will focus on $0 \leqslant |m| \leqslant 2$. In Fig. 3 we compare numerically exact energies to second- and fourth-order perturbation series. Within the perturbative regime, i.e., in low fields $F < 1$, we have verified that a fit of the numerical Stark shift to a polynomial agrees to high precision with the analytical fourth-order
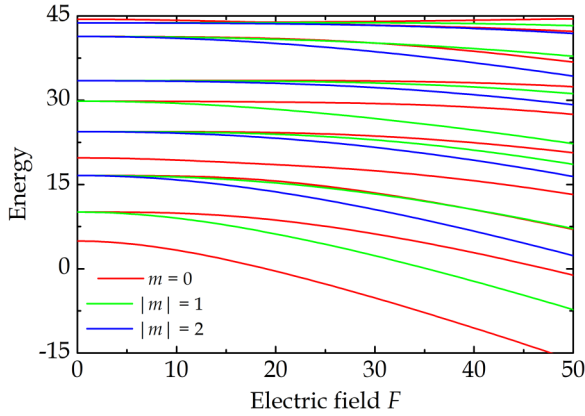
FIG. 2. Numerical diagonalization energy eigenvalues for several m values.

perturbation results. Beyond this regime, as expected, perturbation results deteriorate dramatically, in particular, when the field strength reaches $F \sim 10$. The ground-state correc-
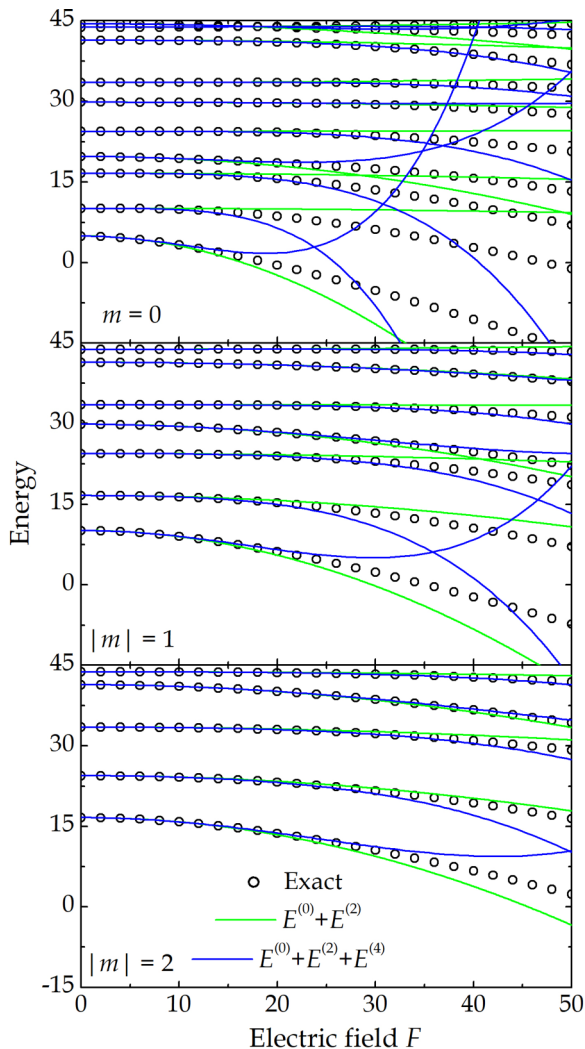

FIG. 3. Comparison of numerical eigenvalues (exact, circles) with low-order perturbation series (green and blue solid lines) for different m quantum numbers.

tion corresponds to a polarizability of $\alpha_{100} = -2E_{100}^{(2)}/F^2 = (3 + 4\pi^2)/12\pi^4 \approx 3.63 \times 10^{-2}$ in agreement with analytical results in Ref. [8] and numerically evaluated sum-over-states expressions [31]. In addition, we find $\beta_{100} = -(405 - 180\pi^2 - 12\pi^4 + 4\pi^6)/135\pi^{10} \approx -10.3 \times 10^{-5}$ as shown in the Appendix. Thus, α and β have opposite signs for the ground state, and this trend is found for all $|m| = l$ states. As shown in Fig. 3, the second-order truncation $E(F) \approx E^{(0)} - \frac{1}{2}\alpha F^2$ (green lines) overestimates the Stark shift for these states. A negative β leads to a fourth-order approximation $E(F) \approx E^{(0)} - \frac{1}{2}\alpha F^2 - \frac{1}{4}\beta F^4$ (blue lines) that partly corrects this behavior. As a consequence, the perturbative Stark shift now underestimates the exact behavior. Eventually, in large fields, the fourth-order approximation tends to large positive values in complete disagreement with the diagonalization results.

In Fig. 4 unperturbed energies and polarizabilities as well as hyperpolarizabilities are collected for the most important low-lying states. These quantities are scaled by n^{-2}, n^2, and n^4, respectively. These scaling factors reflect the asymptotic dependence on n via λ_{ln} in Eqs. (2), (8), and (12). Hence, all three quantities approach constants as n is increased when scaled in this manner. It may be noted that α_{nlm} is positive for all states in the plot while the sign of β_{nlm} varies. In particular, for $|m| = l$, the signs of α_{nlm} and β_{nlm} are always opposite, in agreement with the observation for the $n = 1$ state discussed above. In fact, states with $\alpha_{nlm} < 0$ do exist, as can be verified from Eq. (8), but only for higher m values.

As clearly seen from Fig. 3, the finite perturbation series break down beyond a critical field strength around $F \sim 10$. This observation is intimately tied to the failure of the series to capture the correct high-field behavior. In extreme fields, the electron localizes completely on the surface of the sphere near the "south pole" using the geometry in Fig. 1. This means that the asymptotic energy is simply $E(F \to \infty) \approx -F$. The first correction to this strong-field limit [32] varies as $F^{2/3}$. Such asymptotic behavior is clearly highly nonperturbative and, hence, hard to capture in a perturbation series. A related problem is the high-field Stark effect in the hydrogen atom. There the eigenvalue is really a complex resonance whose imaginary part describes the ionization rate due to field-assisted tunneling out of the Coulomb barrier. The hydrogen resonance varies asymptotically as [28] $E(F \to \infty) \propto (F \ln F)^{2/3} \exp(-i\pi/3)$.

For the hydrogen atom in three and fewer dimensions [1–5], as well as anisotropic surroundings [25], the perturbation series have been successfully resummed using hypergeometric functions of the form $_2F_1(h_1, h_2, h_3, z)$ with z either h_4F^2 or $1 + h_4F^2$. For $z > 1$, one encounters a branch cut of the hypergeometric function that, in turn, becomes complex-valued. Conversely, for all $z < 1$ and h_i real, the function is real-valued and, specifically, $_2F_1(h_1, h_2, h_3, 0) = 1$. One may construct a hypergeometric ansatz that, by construction, leads to the correct second-order expansion by writing

$$E_H(F) = E^{(0)} + E^{(2)} \times {}_2F_1(h_1, h_2, h_3, -h_4F^2). \quad (13)$$

Asymptotically, this ansatz displays a double power form $E_H(F \to \infty) \sim c_1 F^{2(1-h_1)} + c_2 F^{2(1-h_2)}$. Hence, the correct limiting form is ensured if we take $h_1 = 1/2$ and $h_2 = 2/3$.
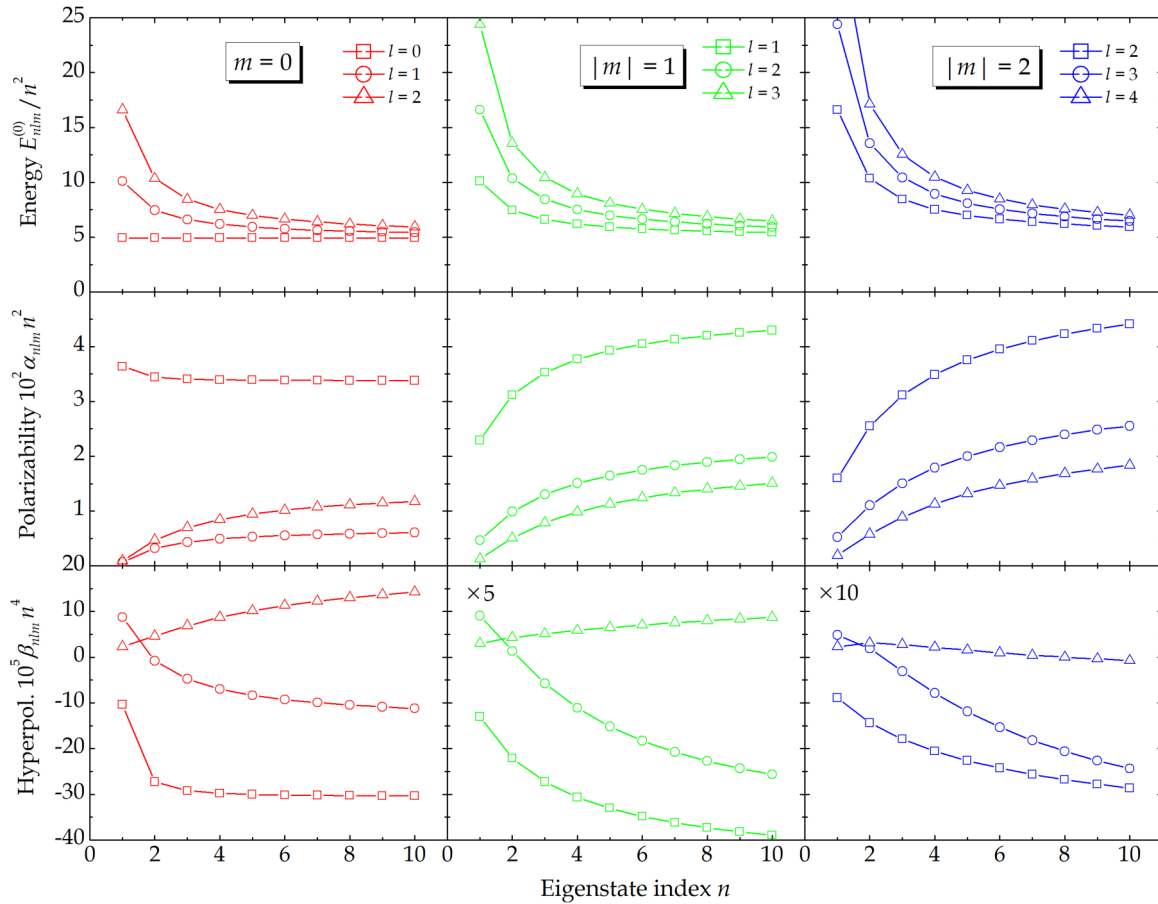
FIG. 4. Energy, polarizability, and hyperpolarizability for low-lying eigenstates as a function of state index n.

Furthermore, we require $c_1 = -1$. Since there are four free parameters h_i in the ansatz, we must formulate one additional requirement to uniquely fix the ansatz. In the present context, it is natural to demand agreement with the fourth-order perturbation expansion; i.e., we set $E_H(F) = E^{(0)} + E^{(2)} + E^{(4)} + O(F^6)$. This eventually leads to the conditions $h_3 = -h_4 E^{(2)} F^2/(3E^{(4)})$ and $E^{(2)}\Gamma(\frac{1}{6})\Gamma(h_3) + F^2\sqrt{h_4}\Gamma(\frac{2}{3})\Gamma(h_3 - \frac{1}{2}) = 0$ that must be solved simultaneously. Note that in writing the hypergeometric argument as $-h_4 F^2$ we have implicitly assumed h_4 positive to ensure a real-valued result. This assumption is, indeed, fulfilled by the solution to the above equations. As alternatives to hypergeometric functions, Padé approximants or more general functions could have been chosen. However, hypergeometrics generally triumph [27] because they possess the physically correct branch cut structure and, moreover, are defined by a small set of parameters, i.e., four, such that only a few terms from low and/or high field expansions are needed to uniquely fix the approximant.

In Fig. 5 the hypergeometric ansatz is tested against perturbative and numerically exact data for the ground state. The perturbative expressions have been carried to 14th order using the series in the Appendix. It is seen, however, that this barely improves the agreement over the second- and fourth-order results. For fields around the critical strength $F \sim 10$, the 14th-order expansion does improve agreement with exact values, as displayed in the inset of Fig. 5. Unfortunately,

however, when the field exceeds $F \approx 15$, the 14th-order series deviates dramatically from the correct behavior. In fact, the second-order series remains the most accurate one in the high-field regime. In contrast, the hypergeometric ansatz remains highly accurate in the entire field range. At low, medium, and high fields, Eq. (13) is superior to the truncated series. This very clearly demonstrates the importance of incorporating high-field information into any approximate form.
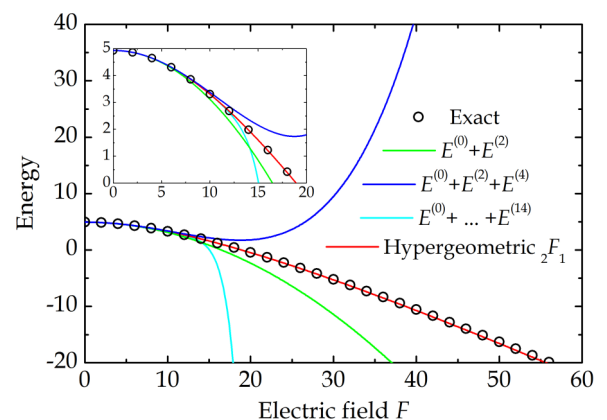

FIG. 5. Comparison of exact diagonalization results (circles) with perturbative expansions (green, blue, and cyan) and hypergeometric ansatz (red line). The inset is a zoom of the low-field regime.

IV. SUMMARY

In the present work, the problem of spherical nanoparticles in strong electric fields has been investigated using a combination of numerical and analytical tools. An analytical perturbation series for the Stark shift has been obtained for general eigenstates. For the ground state, results up to 14th order in the field have been found. While the analytics are in excellent agreement with numerical diagonalization data in the low-field regime, they become highly unreliable above a critical field $F \approx 15 F_0$ with characteristic field $F_0 = \hbar^2/(em_e a^3)$ for a nanoparticle of radius a and effective mass m_e. The correct high-field behavior has been restored using a hypergeometric resummation scheme. In particular, for the ground state, the resummation approach has been shown to outperform even very high-order perturbation series in a wide range of field strengths.

APPENDIX: STARK EFFECT FOR *S*-STATES

The perturbation series for general states E_{nlm} is rather complicated, as indicated by the fourth-order term (12). However, for all *s*-states with $l = m = 0$, a reasonably compact form is found. Hence, introducing $\lambda \equiv \lambda_{0n}$ we find up to eighth order

$$E_{n00}^{(0)} = \frac{\lambda^2}{2}, \quad E_{n00}^{(2)} = -F^2 \frac{3 + 4\lambda^2}{24\lambda^4}, \quad E_{n00}^{(4)} = F^4 \frac{405 - 180\lambda^2 - 12\lambda^4 + 4\lambda^6}{540\lambda^{10}},$$

$$E_{n00}^{(6)} = F^6 \frac{93\,767\,625 - 57\,281\,175\lambda^2 + 8\,221\,500\lambda^4 - 13\,716\lambda^6 - 8928\lambda^8 - 2976\lambda^{10} + 64\lambda^{12}}{272\,160\lambda^{16}(\lambda^2 - 15)},$$

$$E_{n00}^{(8)} = F^8 \frac{1}{61\,236\,000\lambda^{22}(\lambda^2 - 15)^2(2\lambda^2 - 21)} \big\{ -479\,762\,053\,312\,500 + 390\,205\,264\,443\,750\lambda^2$$

$$- 110\,092\,960\,805\,625\lambda^4 + 14\,542\,937\,640\,000\lambda^6 - 872\,103\,665\,925\lambda^8 + 12\,541\,059\,900\lambda^{10}$$

$$+ 486\,980\,100\lambda^{12} + 11\,776\,320\lambda^{14} - 1\,291\,248\lambda^{16} + 42\,432\lambda^{18} - 832\lambda^{20} \big\}. \tag{A1}$$

Closed-form expressions have been obtained to 14th order, but the results are rather lengthy even for *s*-states. Thus, we settle for the numerically evaluated series for the ground state $n = 1$ with $\lambda_{01} = \pi$:

$$E_{100} \approx 4.9348 - 1.8170 \times 10^{-2}F^2 + 2.5808 \times 10^{-5}F^4 - 9.4109 \times 10^{-8}F^6$$

$$+ 4.5149 \times 10^{-10}F^8 - 2.4666 \times 10^{-12}F^{10} + 1.4537 \times 10^{-14}F^{12} - 9.0056 \times 10^{-17}F^{14}. \tag{A2}$$

[1] H. R. Hasse, Proc. Cambridge Philos. Soc. **26**, 542 (1930).

[2] R. J. Damburg and V. V. Kolosov, J. Phys. B **9**, 3149 (1976).

[3] V. Privman, Phys. Rev. A **22**, 1833 (1980).

[4] K. Tanaka, M. Kobashi, T. Shichiri, T. Yamabe, D. M. Silver, and H. J. Silverstone, Phys. Rev. B **35**, 2513 (1987).

[5] T. G. Pedersen, H. Mera, and B. K. Nikolić, Phys. Rev. A **93**, 013409 (2016).

[6] D. A. B. Miller, D. S. Chemla, T. C. Damen, A. C. Gossard, W. Wiegmann, T. H. Wood, and C. A. Burrus, Phys. Rev. Lett. **53**, 2173 (1984).

[7] D. Li, J. Zhang, Q. Zhang, and Q. Xiong, Nano Lett. **12**, 2993 (2012).

[8] T. G. Pedersen, New J. Phys. **19**, 043011 (2017).

[9] Y. Chiba and S. Ohnishi, Phys. Rev. B **38**, 12988 (1988).

[10] J. W. Haus, H. S. Zhou, I. Honma, and H. Komiyama, Phys. Rev. B **47**, 1359 (1993).

[11] S. A. Empedocles and M. G. Bawendi, Science **278**, 2114 (1997).

[12] P. W. Fry, I. E. Itskevich, D. J. Mowbray, M. S. Skolnick, J. J. Finley, J. A. Barker, E. P. O'Reilly, L. R. Wilson, I. A. Larkin, P. A. Maksym, M. Hopkinson, M. Al-Khafaji, J. P. R. David, A. G. Cullis, G. Hill, and J. C. Clark, Phys. Rev. Lett. **84**, 733 (2000).

[13] F. Wang, J. Shan, M. A. Islam, I. P. Herman, M. Bonn, and T. F. Heinz, Nat. Mater. **5**, 861 (2006).

[14] F. Dujardin, E. Feddi, E. Assaid, and A. Oukerroum, Eur. Phys. J. B **74**, 507 (2010).

[15] S. Wu and W. Xia, J. Appl. Phys. **114**, 043709 (2013).

[16] S. Evangelisti, G. L. Bendazzoli, and A. Monari, Theor. Chem. Acc. **126**, 257 (2010).

[17] T. G. Pedersen, Phys. Rev. B **96**, 115432 (2017).

[18] J. J. H. Pijpers, M. T. W. Milder, C. Delerue, and M. Bonn, J. Phys. Chem. C **114**, 6318 (2010).

[19] T. G. Pedersen, Phys. Rev. B **94**, 125424 (2016).

[20] M. Massicotte, F. Vialla, P. Schmidt, M. Lundeberg, S. Latini, S. Haastrup, M. Danovich, D. Davydovskaya, K. Watanabe, T. Taniguchi, V. Fal'ko, K. Thygesen, T. G. Pedersen, and F. H. L. Koppens, Nat. Commun. **9**, 1633 (2018).

[21] A. Dalgarno and J. T. Lewis, Proc. R. Soc. Lond. A **233**, 70 (1955).

[22] H. A. Mavromatis, Am. J. Phys. **59**, 738 (1991).

[23] M. A. Maize, M. A. Antonacci, and F. Marsiglio, Am. J. Phys. **79**, 222 (2011).

[24] T. G. Pedersen, Solid State Commun. **141**, 569 (2007).

[25] T. G. Pedersen, S. Latini, K. S. Thygesen, H. Mera, and B. K. Nikolić, New J. Phys. **18**, 073043 (2016).

[26] U. D. Jentschura, Phys. Rev. A **64**, 013403 (2001).

[27] H. Mera, T. G. Pedersen, and B. K. Nikolić, Phys. Rev. Lett. **115**, 143001 (2015).

[28] I. W. Herbst and B. Simon, Phys. Rev. Lett. **41**, 67 (1978).

[29] M Abramowitz and I. A. Stegun, *Handbook of Mathematical Functions with Formulas, Graphs and Mathematical Tables* (Dover Publications, New York, 1972).

[30] T. G. Pedersen, Phys. Lett. A **382**, 1837 (2018).

[31] B. Billaud, M. Picco, and T.-T. Truong, J. Phys.: Condens. Matter **21**, 395302 (2009).

[32] G. Wei, S. Wang, and G. Yi, Microelectron. J. **39**, 786 (2008).